



Contents lists available at ScienceDirect



# Catalysis Today

journal homepage: [www.elsevier.com/locate/cattod](http://www.elsevier.com/locate/cattod)

## Selective hydrodeoxygenation of lignin-related 4-propylphenol into *n*-propylbenzene in water by Pt-Re/ZrO<sub>2</sub> catalysts

Hidetoshi Ohta <sup>a,b</sup>, Bo Feng <sup>a</sup>, Hirokazu Kobayashi <sup>a</sup>, Kenji Hara <sup>a</sup>, Atsushi Fukuoka <sup>a,\*</sup>

<sup>a</sup> Catalysis Research Center, Hokkaido University, Kita 21 Nishi 10, Kita-ku, Sapporo, Hokkaido 001-0021, Japan

<sup>b</sup> Department of Materials Science and Biotechnology, Graduate School of Science and Engineering, Ehime University, 3 Bunkyo-cho, Matsuyama 790-8577, Japan

### ARTICLE INFO

#### Article history:

Received 8 November 2013

Received in revised form 17 January 2014

Accepted 22 January 2014

Available online xxx

#### Keywords:

Biomass

Hydrodeoxygenation

Lignin model

Aromatic hydrocarbon

Pt catalyst

Water

### ABSTRACT

Bimetallic Pt-Re/ZrO<sub>2</sub> catalysts were developed for the selective hydrodeoxygenation of 4-propylphenol as a lignin model to *n*-propylbenzene in water. The addition of Re to Pt/ZrO<sub>2</sub> improved the catalyst stability and product selectivity. Reaction temperature greatly affected not only reaction efficiency but also product distribution. *n*-Propylbenzene was obtained in up to 73% yield with ca. 80% selectivity. After the reaction, the catalyst was deactivated possibly due to water-induced wrapping of Pt nanoparticles in ZrO<sub>2</sub>. The reaction may involve the hydrogenation of 4-propylphenol to 4-propylcyclohexanol, followed by the dehydration to give 4-propylcyclohexene and the subsequent dehydrogenation to *n*-propylbenzene.

© 2014 Elsevier B.V. All rights reserved.

## 1. Introduction

The use of renewable biomass for the synthesis of petrochemicals is crucial to reduce the dependency on limited reserves of fossil fuels [1–4]. Due to the structure and availability, lignin is considered as a promising resource of aromatic hydrocarbons which are industrially important feedstock for producing a wide variety of useful chemicals such as polymers, pharmaceuticals, agrochemicals and electronic chemicals [5]. Hydrodeoxygenation (HDO) is an important technology for upgrading of lignin and related chemicals into aliphatic [6–9] and aromatic hydrocarbons [10–16]. For the synthesis of aromatic hydrocarbons, conventional sulfided CoMo catalysts show good activity [17–19]; however, they suffer from the deactivation caused by coke formation and in-situ generated water in the HDO reaction [20]. Ni/SiO<sub>2</sub> was developed for the gas-phase conversion of phenol to benzene in mixed aqueous/methanolic solutions, in which product selectivity was greatly dependent on water content [21]. It should be noted that actual lignin and bio-oils always contain plenty of water. Therefore, the development of highly efficient and water-tolerant catalyst system is desirable for

the HDO of lignin and related chemicals into aromatic hydrocarbons.

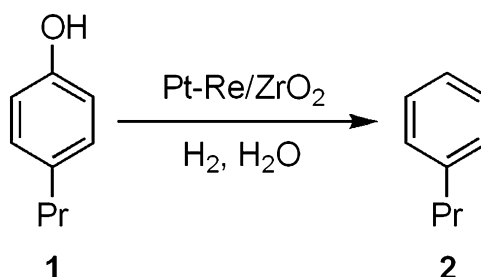
Aqueous-phase HDO of phenols has been extensively investigated in recent years [22–26]. This process is suitable for the conversion of water-containing lignin-related chemicals, and the easy separation of the organic products from the aqueous phase is also beneficial. Pt/C [27] and Ni-Re/ZrO<sub>2</sub> [28] were evaluated in the HDO of phenols into aromatic hydrocarbons in water. However, the yields and selectivities of aromatic products are still insufficient. We previously reported the aqueous-phase conversion of phenols into aliphatic hydrocarbons by Pt/AC (activated carbon) [29,30]. During our continuous efforts to improve the catalyst efficiency, we found that Pt-Re/ZrO<sub>2</sub> catalysts facilitated the HDO of 4-propylphenol (**1**) into *n*-propylbenzene (**2**) with high yields and selectivities (Scheme 1). Herein, we report the details of characterization and catalytic behavior of Pt-Re/ZrO<sub>2</sub> in the aqueous-phase HDO reaction.

## 2. Experimental

### 2.1. General

ZrO<sub>2</sub> (JRC-ZRO-2), TiO<sub>2</sub> (JRC-TIO-4(2)) and CeO<sub>2</sub> (JRC-CEO-2) were supplied by Catalysis Society of Japan. γ-Al<sub>2</sub>O<sub>3</sub> (A-11) was purchased from Nishio Industry and SiO<sub>2</sub> (CAB-O-SIL M-5)

\* Corresponding author. Tel.: +81 11 706 9140; fax: +81 11 706 9139.  
E-mail address: [fukuoka@cat.hokudai.ac.jp](mailto:fukuoka@cat.hokudai.ac.jp) (A. Fukuoka).

**Scheme 1.** Selective conversion of 4-propylphenol **1** to *n*-propylbenzene **2**.

from Acros Organics. These metal-oxide supports were calcined in air at 400 °C for 4 h before use. Activated carbon (activated charcoal Norit SX Ultra, denoted as AC) was purchased from Aldrich and used without further treatment. The following chemicals were purchased and used as received: H<sub>2</sub>PtCl<sub>6</sub>·6H<sub>2</sub>O and HAuCl<sub>4</sub>·4H<sub>2</sub>O from Kanto; NH<sub>4</sub>ReO<sub>4</sub>, SnCl<sub>2</sub>·2H<sub>2</sub>O, Fe(NO<sub>3</sub>)<sub>3</sub>·9H<sub>2</sub>O, PdCl<sub>2</sub>, Na<sub>2</sub>WO<sub>4</sub>·2H<sub>2</sub>O, (NH<sub>4</sub>)<sub>6</sub>Mo<sub>7</sub>O<sub>24</sub>·4H<sub>2</sub>O and Bi(NO<sub>3</sub>)<sub>3</sub>·5H<sub>2</sub>O from Wako; Ga(NO<sub>3</sub>)<sub>3</sub>·nH<sub>2</sub>O and In(NO<sub>3</sub>)<sub>3</sub>·3H<sub>2</sub>O from Junsei; aqueous solution of H<sub>2</sub>IrCl<sub>6</sub> from Furuya Metals; 4-propylphenol, propylbenzene, propylcyclohexane, 4-propylcyclohexanol and 4-propylcyclohexanone from Tokyo Chemical Industry.

## 2.2. Preparation of catalysts

All the catalysts were prepared by the co-impregnation method and Pt loading was kept at 2 wt%. For example, the procedure for preparing Pt-Re/ZrO<sub>2</sub> (Pt/Re molar ratio 3) was as follows: aqueous solutions of H<sub>2</sub>PtCl<sub>6</sub> (0.211 mmol in 10 mL water) and NH<sub>4</sub>ReO<sub>4</sub> (0.070 mmol in 300 μL water) were sequentially added to a mixture of ZrO<sub>2</sub> (2.00 g) and water (30 mL) with continuous stirring. The reaction mixture was stirred at room temperature for 15 h, evaporated to dryness and dried under vacuum. The sample was calcined in a fixed-bed flow reactor with O<sub>2</sub> (30 mL min<sup>-1</sup>) at 400 °C for 2 h, then reduced with H<sub>2</sub> (30 mL min<sup>-1</sup>) at 400 °C for 2 h to give Pt-Re/ZrO<sub>2</sub> catalyst. For Pt-Re/AC, only H<sub>2</sub> reduction was performed after drying the impregnated sample. The prepared catalysts were then exposed to air at room temperature for their passivation.

## 2.3. Catalyst characterization

Powder X-ray diffraction (XRD) patterns were recorded on a Rigaku MiniFlex using Cu K $\alpha$  radiation ( $\lambda = 0.15418$  nm) at 30 kV and 15 mV. N<sub>2</sub> adsorption–desorption analyses were performed at –196 °C with a BEL Japan BELSORP-mini II after heating the samples at 120 °C under vacuum for 2 h. Specific surface areas of samples were calculated according to the Brunauer–Emmett–Teller (BET) method. Pore size distributions were estimated by the Barrett–Joyner–Halenda (BJH) method. X-ray photoelectron spectroscopy (XPS) was performed with a JEOL JPC-9010MC using Mg K $\alpha$  radiation (1253.6 eV) at 100 W and a pass energy of 20 eV. The binding energies were calibrated using adventitious carbon (C<sub>1s</sub> peak at 284.8 eV). Pt L<sub>3</sub>- and Re L<sub>3</sub>-edge X-ray absorption fine structure (XAFS) was measured at room temperature in the transmission mode with a synchrotron radiation (ring energy 2.5 GeV, 450 mA) through a Si(1 1 1) double-crystal monochromator at BL-12 C beam line on KEK-PF (Proposal No. 2013G222). The measurement was conducted in the quick XAFS mode (20 s for 1 scan) and repeated 64 times to improve the signal–noise ratio. Transmission electron microscopy (TEM) was conducted with a JEOL JEM-2000ES at an accelerating voltage of 200 kV. Energy dispersive X-ray spectroscopy (EDX) was measured on a Shimadzu Rayny EDX-720. CO chemisorption was carried out with a BEL Japan BELCAT-A. Prior to the chemisorption experiment, a sample was reduced by H<sub>2</sub> at

**Table 1**  
Structural parameters of catalysts.

Catalyst	$S_{\text{BET}}$ (m <sup>2</sup> g <sup>-1</sup> ) <sup>a</sup>	$d_p$ (nm) <sup>b</sup>	$d_{\text{TEM}}$ (nm) <sup>c</sup>
ZrO <sub>2</sub>	90	3.3	—
Pt/ZrO <sub>2</sub>	72	3.7	— <sup>f</sup>
Pt-Re/ZrO <sub>2</sub> <sup>d</sup>	74	3.3	— <sup>f</sup>
Pt-Re/ZrO <sub>2</sub> after the reaction <sup>e</sup>	65	3.7	1.7 ± 0.2

<sup>a</sup> BET surface area.

<sup>b</sup> Average pore diameter.

<sup>c</sup> Mean diameter of Pt particle by TEM analysis.

<sup>d</sup> Pt/Re molar ratio 3.

<sup>e</sup> After the reaction in entry 18, **Table 3**.

<sup>f</sup> Pt nanoparticles were not observed.

200 °C for 100 min, followed by cooling to 50 °C under He flow. The chemisorption of CO was performed at 50 °C (with 10% CO in He), where an equilibrium was assumed when no further CO adsorption was observed.

## 2.4. Catalytic HDO of 4-propylphenol in water

A typical procedure: 4-propylphenol (5.0 mmol, 681 mg), catalyst (2 wt% Pt loading, 98 mg) and water (40 mL) were charged in a well dried high-pressure batch reactor (OM Lab-Tech MMJ-100, SUS316, 100 mL). After pressurization with H<sub>2</sub> to 2 MPa at room temperature, the reactor was heated to the desired reaction temperature with continuous stirring at 600 rpm. Then, the reactor was kept at the reaction temperature for 1 h. After cooling to room temperature, the reaction mixture was extracted with ethyl acetate and the organic layer was analyzed by GC and GC-MS using 2-isopropylphenol as an internal standard. GC analyses were carried out using a Shimadzu GC-14B equipped with an integrator (C-R8A) with a capillary column (HR-1, 0.25 mm i.d. × 50 m). GC-MS analyses were measured by a Shimadzu GC-2010/PARVUM2 equipped with the same column. The catalyst was recovered by centrifugation, followed by washing with ethyl acetate and dried in an oven at 120 °C for 2 h. The recovered catalyst was reused in the next reaction.

For the time-course study, many batch reactions at different time were performed separately. Here, the reaction time “0” was defined as the time when the temperature of the reaction mixture just reached the reaction temperature.

## 3. Results and discussion

### 3.1. Characterization of Pt/ZrO<sub>2</sub> and Pt-Re/ZrO<sub>2</sub> catalysts

Characterization of ZrO<sub>2</sub>, Pt/ZrO<sub>2</sub>, and Pt-Re/ZrO<sub>2</sub> were performed by N<sub>2</sub> adsorption and XRD analyses. The structural parameters were summarized in **Table 1**. ZrO<sub>2</sub>, Pt/ZrO<sub>2</sub>, and Pt-Re/ZrO<sub>2</sub> have BET surface areas of 72–90 m<sup>2</sup> g<sup>-1</sup> with a pore size of 3.3–3.7 nm. In the XRD patterns of these samples, large peaks of monoclinic ZrO<sub>2</sub> phase and a small peak of tetragonal ZrO<sub>2</sub> phase were observed (**Fig. 1(a)–(c)**). TEM and XPS measurements of Pt/ZrO<sub>2</sub> and Pt-Re/ZrO<sub>2</sub> were conducted to estimate the metal particle size and the electronic states of the Pt and Re species. The Pt nanoparticles were not observed on the TEM images of Pt/ZrO<sub>2</sub> and Pt-Re/ZrO<sub>2</sub>, suggesting the high dispersion of Pt nanoparticles (**Fig. 2(a)** and (**b**)). The XPS analyses of Pt/ZrO<sub>2</sub> and Pt-Re/ZrO<sub>2</sub> showed that Pt existed as Pt(0) and oxidized Pt species on the catalyst surface (**Fig. 3**). The peaks in Pt<sub>4f</sub> region of Pt-Re/ZrO<sub>2</sub> (Pt<sub>4f</sub>/<sub>2</sub> = 72.7 eV) were observed at higher binding energy than that of Pt/ZrO<sub>2</sub> (Pt<sub>4f</sub>/<sub>2</sub> = 71.7 eV), suggesting the interaction of Pt with Re [31,32]. The Re<sub>4f</sub> peaks of Pt-Re/ZrO<sub>2</sub> indicate that the major Re species is Re(6+); however, more information was not obtained due

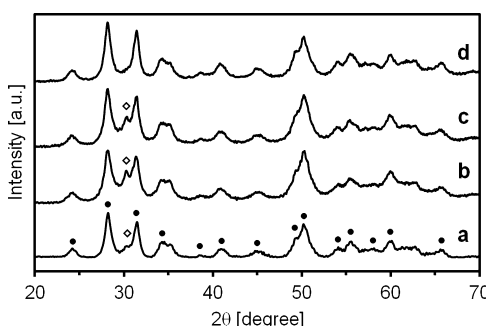


**Fig. 1.** XRD patterns of (a) ZrO<sub>2</sub>; (b) Pt/ZrO<sub>2</sub>; (c) Pt-Re/ZrO<sub>2</sub>; (d) Pt-Re/ZrO<sub>2</sub> after the reaction (Table 3, entry 18). Circles (●): monoclinic ZrO<sub>2</sub>. Diamond (◊): tetragonal ZrO<sub>2</sub>.

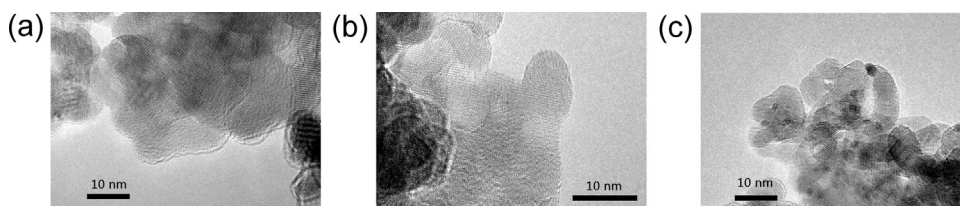
to the overlapping of the peaks of Re<sub>4f</sub> and Zr<sub>4s</sub> as well as the low Re loading (0.67 wt%).

XAFS spectra were measured to elucidate the oxidation states of Pt and Re species on Pt-Re/ZrO<sub>2</sub> (Fig. 4). With regard to Pt L<sub>3</sub>-edge X-ray near edge structure (XANES), Pt-Re/ZrO<sub>2</sub> provided a larger white line than that of Pt foil at 11565 eV. This result also shows that Pt is partially oxidized as indicated by the XPS study. A curve fitting suggested that ca. 25% fraction of Pt species was oxides and

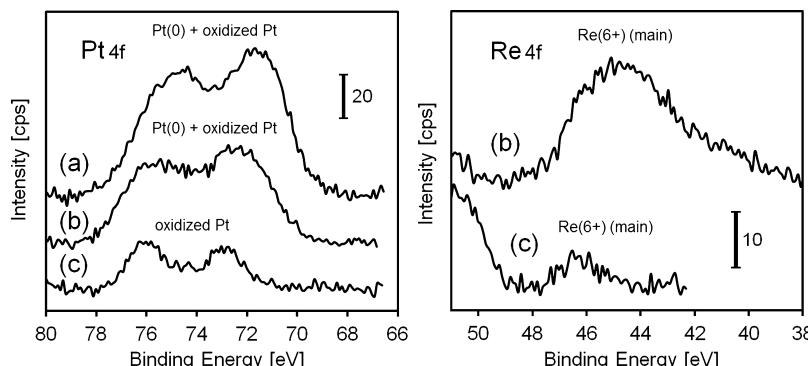
the remaining part was metal in the catalyst, using the spectra of Pt foil and PtO<sub>2</sub> [33]. As to Re L<sub>3</sub>-edge, intensity of the white line for Pt-Re/ZrO<sub>2</sub> corresponded to those for tetra- to hexa-valent oxides [34,35]. These oxide species could be formed by the passivation in the catalyst preparation, due to high dispersion of metals. It is known that Ru, also a precious metal, particles less than 2 nm is converted to RuO<sub>2</sub>·2H<sub>2</sub>O in air even at room temperature [36]. Note that these oxides can be reduced under reaction conditions in the presence of H<sub>2</sub> to work as catalysts [37].

### 3.2. HDO of 4-propylphenol by supported Pt catalysts

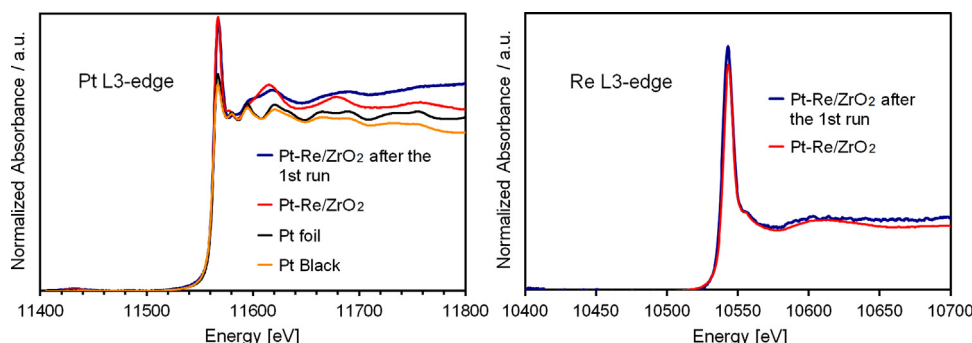
HDO of 4-propylphenol (**1**) was examined with various Pt catalysts supported on ZrO<sub>2</sub> in water at 300 °C for 1 h under 2 MPa H<sub>2</sub> (Table 2). Monometallic Pt/ZrO<sub>2</sub> gave propylbenzene (**2**) in 40% yield (65% selectivity) with aliphatic hydrocarbons (**3+4**; 15% selectivity) and oxygenates (**5+6**; 16% selectivity) (entry 1). The use of bimetallic catalysts greatly affected the product distribution. Pt-Re/ZrO<sub>2</sub> converted **1** into **2** in 57% yield with 85% selectivity, where **5** and **6** were formed in only 1% selectivity (entry 2). The addition of Sn, Ir, Ga, and Fe had little effect on the catalytic performance of Pt/ZrO<sub>2</sub> (entries 3–6). Au, Pd, W and In gave higher yields of **3–6**, leading to a decrease in the selectivity of **2** (entries 7–10). By contrast, Pt-Mo/ZrO<sub>2</sub> and Pt-Bi/ZrO<sub>2</sub> showed much lower activity



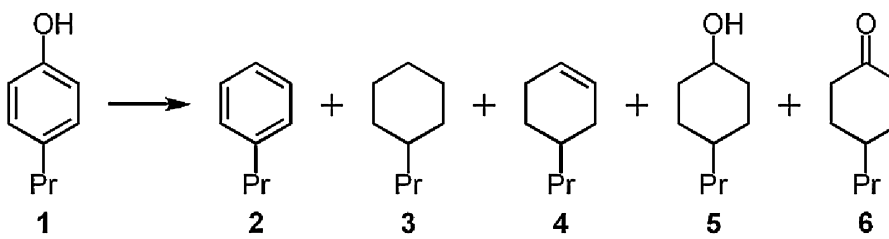
**Fig. 2.** TEM images of (a) Pt/ZrO<sub>2</sub>; (b) Pt-Re/ZrO<sub>2</sub>; (c) Pt-Re/ZrO<sub>2</sub> after the reaction (Table 3, entry 18).



**Fig. 3.** XPS spectra for the Pt<sub>4f</sub> and Re<sub>4f</sub> regions of (a) Pt/ZrO<sub>2</sub>; (b) Pt-Re/ZrO<sub>2</sub>; (c) Pt-Re/ZrO<sub>2</sub> after the reaction (Table 3, entry 18).



**Fig. 4.** Pt L<sub>3</sub>-edge and Re L<sub>3</sub>-edge XANES spectra of Pt-Re/ZrO<sub>2</sub> catalysts.

**Table 2**Aqueous-phase HDO of 4-propylphenol **1** by supported Pt catalysts<sup>a</sup>.

Entry	Catalyst	Conversion (%)	Yield (selectivity) <sup>b</sup> (%)				
			<b>2</b>	<b>3</b>	<b>4</b>	<b>5</b>	<b>6</b>
1	Pt/ZrO <sub>2</sub>	62	40 (65)	8 (13)	1 (2)	8 (13)	2 (3)
2	Pt-Re/ZrO <sub>2</sub>	67	57 (85)	9 (13)	0.1 (0.1)	1 (1)	0.2 (0.3)
3	Pt-Sn/ZrO <sub>2</sub>	61	44 (72)	10 (16)	0.1 (0.2)	3 (5)	0
4	Pt-Ir/ZrO <sub>2</sub>	65	43 (66)	9 (14)	2 (3)	4 (6)	2 (3)
5	Pt-Ga/ZrO <sub>2</sub>	58	39 (67)	8 (14)	1 (2)	2 (3)	3 (5)
6	Pt-Fe/ZrO <sub>2</sub>	54	34 (63)	7 (13)	1 (2)	4 (7)	2 (4)
7	Pt-Au/ZrO <sub>2</sub>	63	37 (59)	11 (17)	2 (3)	4 (6)	5 (8)
8	Pt-Pd/ZrO <sub>2</sub>	59	33 (56)	9 (15)	2 (3)	14 (24)	1 (2)
9	Pt-W/ZrO <sub>2</sub>	66	33 (50)	7 (11)	2 (3)	5 (8)	14 (21)
10	Pt-In/ZrO <sub>2</sub>	51	24 (47)	9 (18)	2 (4)	6 (12)	1 (2)
11	Pt-Mo/ZrO <sub>2</sub>	8.8	4.9 (56)	0.9 (10)	0.3 (3)	0.9 (10)	1.8 (21)
12	Pt-Bi/ZrO <sub>2</sub>	4.4	2.2 (50)	0.4 (9)	0.2 (5)	0.6 (14)	1.0 (23)
13	Pt-Re/TiO <sub>2</sub>	58	41 (71)	13 (22)	0.3 (1)	1 (2)	1 (2)
14	Pt-Re/Al <sub>2</sub> O <sub>3</sub>	41	27 (66)	4 (10)	1 (2)	4 (10)	1 (3)
15	Pt-Re/CeO <sub>2</sub>	45	24 (53)	11 (24)	2 (4)	4 (9)	0
16	Pt-Re/SiO <sub>2</sub>	8.1	1.3 (16)	0.4 (5)	0.1 (1)	1.8 (22)	3.7 (46)
17	Pt-Re/AC	90	3 (3)	17 (19)	0	62 (69)	0

<sup>a</sup> Reaction conditions: 4-propylphenol **1** (5.0 mmol, 681 mg), catalyst (98 mg, 2 wt% Pt loading, Pt/M molar ratio 3), water (40 mL), initial H<sub>2</sub> pressure at RT = 2 MPa, 300 °C, 1 h, 600 rpm.

<sup>b</sup> Selectivity is based on the substrate conversion.

(4–9% conversion) and selectivity of **2** (50–56%) (entries 11 and 12). Catalyst supports have a significant influence on the catalytic activity in this reaction. Pt-Re catalysts supported on TiO<sub>2</sub>, Al<sub>2</sub>O<sub>3</sub>, and CeO<sub>2</sub> were moderately active for the reaction, affording lower yields of **2** than Pt-Re/ZrO<sub>2</sub> (entries 13–15). In sharp contrast, Pt-Re/SiO<sub>2</sub> was less active with only 8% conversion, giving oxygenates **5** and **6** as major products (entry 16). In addition, Pt-Re/AC greatly facilitated the conversion of **1** into **3** (17% yield) and **5** (62% yield) (entry 17). Among the catalysts tested, Pt-Re/ZrO<sub>2</sub> was found to be the most effective catalyst in the selective HDO of **1** into **2** in water.

To further optimize the reaction conditions, Pt/Re molar ratio and reaction temperature were investigated. Fig. 5 shows the influence of different Pt/Re ratio on the catalytic performance. The conversions were nearly identical in the Pt/Re ratios of 1–4, but the yield and selectivity of **2** were affected by the Pt/Re ratio. The Pt/Re ratio of 3 was the best composition for the production of **2**.

Reaction temperature had significant effect on the selectivity of the products (Fig. 6). The reaction was completed at 260 °C to give **2** and **3** in 60% and 39% yields, respectively. The selectivity of **2** was increased at higher temperatures, and the highest yield of **2** was obtained at 280 °C (73% yield, 81% selectivity). Decrease in the conversion of **1** at 300 °C may be attributed to the dehydrogenation of initially formed **5** into **1** (vide infra).

The recyclability of Pt-Re/ZrO<sub>2</sub> was evaluated in the HDO of **1** at 280 °C (Table 3). After the 1st run (entry 18), the catalyst was recovered by centrifugation and successively subjected to the next reaction. However, the catalytic activity was dramatically reduced to give trace amounts of products (entry 19). Pt/ZrO<sub>2</sub> and Pt-Re/TiO<sub>2</sub>, which showed good catalytic activity in Table 2, were also employed in the reuse experiments; however, the catalytic activities were completely lost in the 2nd runs (entries 21–24). To find out the cause of catalyst deactivation, the recovered

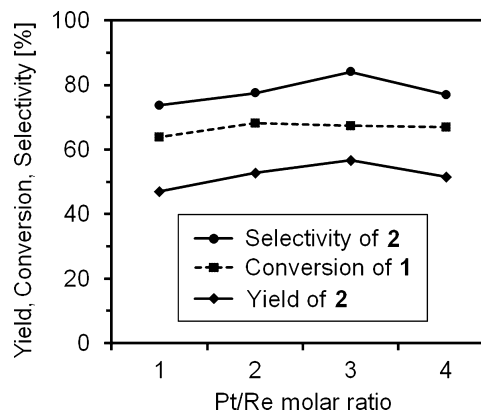


**Fig. 5.** Influence of Pt to Re molar ratio on the HDO of 4-propylphenol **1**. Reaction conditions: see entry 2 in Table 2.

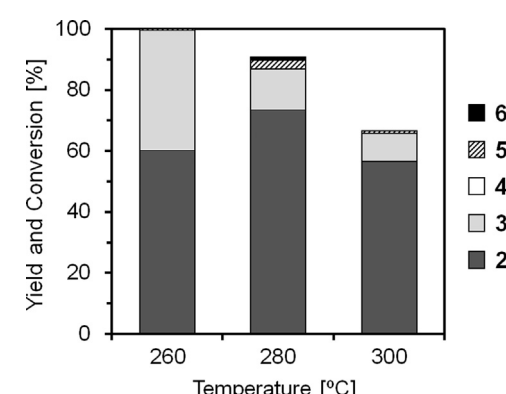


**Fig. 6.** HDO of 4-propylphenol **1** by Pt-Re/ZrO<sub>2</sub> at different reaction temperatures. Reaction conditions: see entry 2 in Table 2.

**Table 3**Reuse experiments of Pt-Re/ZrO<sub>2</sub> in the HDO of 4-propylphenol **1**.<sup>a</sup>

Entry	Run	Conversion (%)	Yield (%)				
			2	3	4	5	6
18	1st	91	73	13	0.1	3	1
19	2nd	1.4	0.3	0	0	0.8	0.3
20 <sup>b</sup>	2nd	1.6	0.2	0	0	0.8	0.6
21 <sup>c</sup>	1st	71	47	13	2	3	4
22 <sup>c</sup>	2nd	2.5	0	0	0	0.2	0
23 <sup>d</sup>	1st	71	44	17	0	10	0
24 <sup>d</sup>	2nd	0.1	0	0	0	0.1	0
25 <sup>e</sup>	1st	100	0	>99	0	0	0
26 <sup>e</sup>	2nd	100	0	84	0	0	0

<sup>a</sup> Reaction conditions: 4-propylphenol **1** (5.0 mmol, 681 mg), Pt-Re/ZrO<sub>2</sub> (98 mg, 2 wt% Pt loading, Pt/Re molar ratio 3), water (40 mL), initial H<sub>2</sub> pressure at RT = 2 MPa, 280 °C, 1 h, 600 rpm.

<sup>b</sup> Regenerated catalyst after the 1st run (entry 18) was used. Regeneration conditions: O<sub>2</sub> calcination at 400 °C for 2 h, then H<sub>2</sub> reduction at 400 °C for 2 h.

<sup>c</sup> Pt/ZrO<sub>2</sub> catalyst was used.

<sup>d</sup> Pt-Re/TiO<sub>2</sub> catalyst was used.

<sup>e</sup> Without water.

Pt-Re/ZrO<sub>2</sub> catalyst after the 1st run was analyzed by EDX, XRD, XPS, XAFS, TEM and adsorption of N<sub>2</sub> and CO. First, no leaching of Pt was observed by EDX analysis. The BET surface areas and pore sizes were slightly changed before and after the reaction (Table 1). The XRD pattern of the recovered catalyst showed the disappearance of the peak of tetragonal ZrO<sub>2</sub> phase observed in the fresh catalysts, suggesting the structural change of ZrO<sub>2</sub> support during the reaction (Fig. 1(d)). The XPS spectrum of spent Pt-Re/ZrO<sub>2</sub> is typically shown in Fig. 3(c). In the XPS study, clear decrease of the peak intensities in Pt<sub>4f</sub>, Zr<sub>3d</sub> and Re<sub>4f</sub> regions and increase in C<sub>1s</sub> region were observed. It implies that coke is formed on the catalyst surface. The Pt<sub>4f</sub> peaks showed that the surface Pt(0) was oxidized. On the other hand, the Re<sub>4f</sub> peak suggests that Re(6+) still exists as a major Re species. Pt L3- and Re L3-edge XAFS measurements provided similar spectra for fresh and spent Pt-Re/ZrO<sub>2</sub> catalysts, showing that the bulk phase of Pt nanoparticles was not affected under the reaction conditions (Fig. 4). The TEM analyses of spent Pt-Re/ZrO<sub>2</sub> showed the sintering of the Pt nanoparticles, but the Pt particle size was still small (1.7 nm) (Table 1; Fig. 2(c)). In contrast to the result of TEM analysis, CO chemisorption of spent Pt-Re/ZrO<sub>2</sub> provided larger Pt particle size of 8.0 nm. This underestimation of Pt dispersion might be due to the coke formation. These results suggest that the deactivation of Pt-Re/ZrO<sub>2</sub> might be due to the coke formation, the oxidation of Pt(0), or sintering of Pt. To check the first two possibilities, the recovered catalyst after the 1st run was regenerated at 400 °C using O<sub>2</sub> followed by H<sub>2</sub> reduction and then used in the next run. However, the reaction gave almost no products (entry 20). It is indicated that the deactivation is not attributed

**Table 4**Control experiments with Pt-Re/ZrO<sub>2</sub> catalyst<sup>a</sup>.

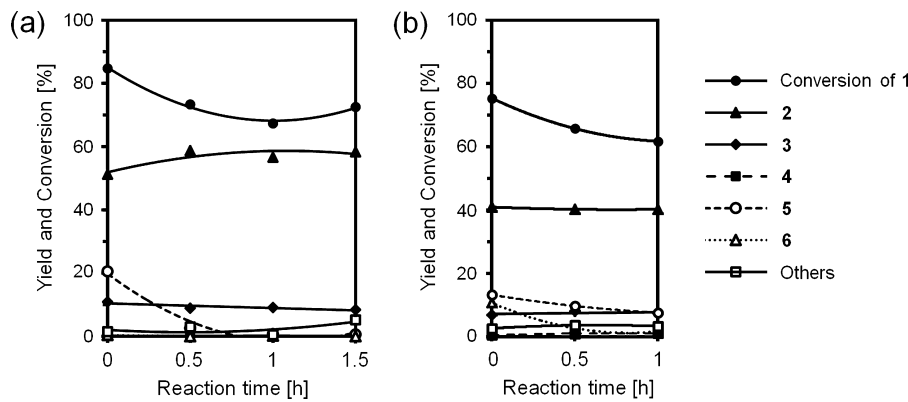
Entry	Substrate	Conversion (%)	Yield (%)				
			1	2	3	4	5
27	2	12	0	—	12	0	0
28	3	2.8	0	2.3	—	0.3	0
29	5	98	4	72	19	0	—

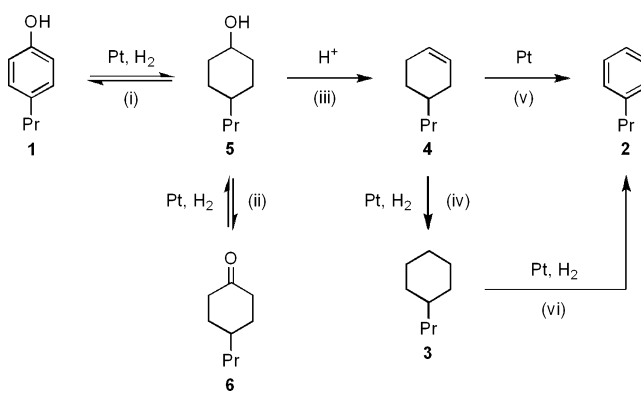
<sup>a</sup> Reaction conditions: substrate (5.0 mmol), Pt-Re/ZrO<sub>2</sub> (98 mg, 2 wt% Pt loading, Pt/Re molar ratio 3), water (40 mL), initial H<sub>2</sub> pressure at RT = 2 MPa, 300 °C, 1 h, 600 rpm.

to the coke formation or the oxidation of Pt(0) species. A control experiment was carried out: Pt-Re/ZrO<sub>2</sub> was pretreated at the reaction conditions (2 MPa H<sub>2</sub>, 280 °C, H<sub>2</sub>O, 1 h) without **1**, then it was used for the HDO of **1**. As a result, the catalyst was also deactivated (1% conversion), indicating that the catalyst was not stable under the reaction conditions. Besides, when the reaction was performed without water solvent, **3** was obtained as a sole product and the catalyst was reusable in the 2nd run with slight loss of activity (entries 25 and 26). These results suggest that high-temperature water plays a key role in the deactivation. The Pt sintering would not be the main cause of deactivation because the Pt particle size is still small (<2 nm). Perhaps, the catalyst deactivation is due to the water-induced wrapping of Pt nanoparticles by ZrO<sub>2</sub> like the SMSI phenomenon [38].

The time-course of the HDO of **1** at 300 °C was shown in Fig. 7. As shown in Fig. 7(a), Pt-Re/ZrO<sub>2</sub> gave 85% conversion even at 0 h, affording **2** (51% yield), **3** (11%), **4** (0.2%), **5** (21%) and **6** (0.4%). Interestingly, the conversion of **1** and the amount of **5** decreased with reaction time, suggesting the dehydrogenation of **5** into **1**. The yield of **2** also increased by time, and the highest yield was obtained after 1 h (57%, entry 2 in Table 2). In contrast, the amount of **3** was kept constant during the reaction. It is suggested that **3** was formed during the temperature rise from room temperature to 300 °C. The HDO by Pt/ZrO<sub>2</sub> showed a similar time-course, but the yield of **2** did not change during the reaction probably due to the catalyst deactivation (Fig. 7(b)). These results indicated that the addition of Re improved the durability of Pt/ZrO<sub>2</sub> catalyst. Probably, the Re species prevent the Pt sintering during the reaction, which is consistent with the results of TEM analysis of spent Pt-Re/ZrO<sub>2</sub> (Table 1).

To gain further insight into the reaction pathways from **1** to **2**, control experiments were carried out with Pt-Re/ZrO<sub>2</sub> catalyst at 300 °C (Table 4). The reaction of **2** afforded **3** in 12% yield via the hydrogenation of aromatic ring (entry 27). **3** was converted only in 3%, giving small amounts of **2** and **4** (entry 28). It is clearly indicated that the dehydrogenation of **3** into **2** was a minor pathway in the HDO of **1**. As shown in entry 29, Pt-Re/ZrO<sub>2</sub> greatly promoted the reaction of **5** to give **1** (4%), **2** (72%) and **3** (19%). There

**Fig. 7.** Time-course of the HDO of 4-propylphenol **1** at 300 °C by (a) Pt-Re/ZrO<sub>2</sub> and (b) Pt/ZrO<sub>2</sub>. Reaction conditions: see entries 1 and 2 in Table 2.

**Fig. 8.** Proposed reaction pathways.

are two probable reaction pathways for the conversion of **5** into **2**. One is the dehydrogenation of **5** to **1** followed by the C—O bond hydrogenolysis of **1** to **2**. The other is the dehydration of **5** to **4** followed by the dehydrogenation of **4** to **2**. The direct C—O bond hydrogenolysis may be difficult because of the high bond dissociation energy of C<sub>aromatic</sub>—OH bond (468 kJ/mol) [39]. In contrast, we [29,30] and other groups [40–42] reported that alcohols were dehydrated to the corresponding alkenes by in-situ generated protons from high-temperature water ( $pK_w = 12$  at  $300^\circ\text{C}$ ) [43]. In addition, we also found that the HDO of **1** into **2** by Ni-Re/ZrO<sub>2</sub> under similar conditions involved the dehydration of **5** to **4** and subsequent dehydrogenation of **4** to **2** [28]. Therefore, we can assume that the present reaction involves the dehydration-dehydrogenation pathway.

**Fig. 8** shows the proposed reaction pathway for the aqueous-phase HDO of **1** by Pt-Re/ZrO<sub>2</sub>. First step is (i) hydrogenation of **1** to **5**, in which the reverse reaction is favorable at high temperature. Then, the reaction proceeds through (ii) dehydrogenation of **5** to **6**, (iii) acid-catalyzed dehydration of **5** to **4**, (iv) hydrogenation of **4** to **3**, (v) dehydrogenation of **4** to **2** and (vi) dehydrogenation of **3** to **2**. Typical HDO reaction of phenols into aromatics proceeds via the direct hydrogenolysis of phenolic C—O bond, which generally requires high temperature over  $300^\circ\text{C}$  [3]. The present reaction involving the pathways (i), (iii) and (v) can be performed even at  $280^\circ\text{C}$  with high efficiency. Based on the similar mechanism, Rinaldi has recently reported the selective HDO of phenol to benzene by using Raney Ni and H-BEA under mild conditions ( $160^\circ\text{C}$ ); however, alkane was used as the solvent and *i*-PrOH as a H-source [44]. The present results may lead to the development of the aqueous-phase HDO of phenols to aromatics by using H<sub>2</sub> gas under mild conditions.

#### 4. Conclusions

We have developed a bimetallic Pt-Re/ZrO<sub>2</sub> catalyst for the aqueous-phase HDO of lignin-related **1** into **2**. The addition of Re to Pt/ZrO<sub>2</sub> improved the catalyst stability and selectivity of **2**. **3** was formed as a major by-product during the temperature rise. Therefore, the improvement of heating method may lead to further increase in the selectivity of **2**. The catalyst was deactivated possibly due to water-induced wrapping of Pt nanoparticles in ZrO<sub>2</sub>. The reaction may involve the dehydration of **5** to **4** and the subsequent dehydrogenation of **4** to **2**. Further investigation of the durable HDO catalysts for the production of **2** in water is now under study.

#### Acknowledgements

This work was supported by a Grant-in-Aid for Scientific Research (KAKENHI, 24760633) from the Japan Society for the Promotion of Science (JSPS). We would like to thank Mr. O. Kawabata for the analysis of XAFS spectra.

#### References

- [1] G.W. Huber, S. Iborra, A. Corma, Chem. Rev. 106 (2006) 4044–4098.
- [2] J.C.S. Ruiz, R. Luque, A.S. Escribano, Chem. Soc. Rev. 40 (2011) 5266–5281.
- [3] P. Bi, Y. Yuan, M. Fan, P. Jiang, Q. Zhai, Q. Li, Bioresource Technol. 136 (2013) 222–229.
- [4] H. Kobayashi, A. Fukuoka, Green Chem. 15 (2013) 1740–1763.
- [5] J. Zakzeski, P.C.A. Bruijnhincx, A.L. Jongerius, B.M. Weckhuysen, Chem. Rev. 110 (2010) 3552–3599.
- [6] V.A. Yakovlev, S.A. Khromova, O.V. Sherstyuk, V.O. Dundich, D. Yu Ermakov, V.M. Novopashina, M. Yu Lebedev, O. Bulavchenko, V.N. Parmon, Catal. Today 144 (2009) 362–366.
- [7] N. Yan, Y. Yuan, R. Dykeman, Y. Kou, P.J. Dyson, Angew. Chem. Int. Edit. 49 (2010) 5549–5553.
- [8] W. Wang, Y. Yang, H. Luo, H. Peng, F. Wang, Ind. Eng. Chem. Res. 50 (2011) 10936–10942.
- [9] C.V. Loricera, P. Castaño, A.I. Molina, I. Hita, A. Gutiérrez, J.M. Arandes, J.L.G. Fierro, B. Pawelec, Green Chem. 14 (2012) 2759–2770.
- [10] R.K.M.R. Kallury, W.M. Restivo, T.T. Tidwell, D.G.B. Boocock, A. Crimi, J. Douglas, J. Catal. 96 (1985) 535–543.
- [11] V.M.L. Whiffen, K.J. Smith, Energy Fuels 24 (2010) 4728–4737.
- [12] M.Á. González-Borja, D.E. Resasco, Energy Fuels 25 (2011) 4155–4162.
- [13] H.Y. Zhao, D. Li, P. Bui, S.T. Oyama, Appl. Catal. A: Gen. 391 (2011) 305–310.
- [14] R.N. Olcese, M. Bettahar, D. Petitjean, B. Malaman, F. Giovanella, A. Dufour, Appl. Catal. B: Environ. 115–116 (2012) 63–73.
- [15] P.T.M. Do, A.J. Foster, J. Chen, R.F. Lobo, Green Chem. 14 (2012) 1388–1397.
- [16] H.W. Park, U.G. Hong, Y.J. Lee, I.K. Song, Catal. Commun. 20 (2012) 89–93.
- [17] B.S. Gevert, J.E. Otterstedt, F.E. Massoth, Appl. Catal. 31 (1987) 119–131.
- [18] E. Laurent, B. Delmon, Ind. Eng. Chem. Res. 32 (1993) 2516–2524.
- [19] Y. Yang, A. Gilbert, C. Xu, Appl. Catal. A: Gen. 360 (2009) 242–249.
- [20] T.R. Viljava, R.S. Komulainen, A.O.I. Krause, Catal. Today 60 (2000) 83–92.
- [21] E.J. Shin, M.A. Keane, Ind. Eng. Chem. Res. 39 (2000) 883–892.
- [22] C. Zhao, Y. Kou, A.A. Lemonidou, X. Li, J.A. Lercher, Angew. Chem. Int. Edit. 48 (2009) 3987–3990.
- [23] D.Y. Hong, S.J. Miller, P.K. Agrawal, C.W. Jones, Chem. Commun. 46 (2010) 1038–1040.
- [24] C. Zhao, J.A. Lercher, Angew. Chem. Int. Edit. 51 (2012) 5935–5940.
- [25] C. Zhao, J.A. Lercher, ChemCatChem 4 (2012) 64–68.
- [26] J. Chen, J. Huang, L. Chen, L. Ma, T. Wang, U.I. Zakai, ChemCatChem 5 (2013) 1598–1605.
- [27] H. Wan, R.V. Chaudhari, B. Subramaniam, Top. Catal. 55 (2012) 129–139.
- [28] B. Feng, H. Kobayashi, H. Ohta, A. Fukuoka, J. Mol. Catal. A: Chem., doi: 10.1016/j.molcata.2013.09.025.
- [29] H. Ohta, H. Kobayashi, K. Hara, A. Fukuoka, Chem. Commun. 47 (2011) 12209–12211.
- [30] H. Kobayashi, H. Ohta, A. Fukuoka, Catal. Sci. Technol. 2 (2012) 869–883.
- [31] E.L. Kunkes, D.A. Simonetti, J.A. Dumesic, W.D. Pyrz, L.E. Murillo, J.G. Chen, D.J. Buttrey, J. Catal. 260 (2008) 164–177.
- [32] L. Zhang, A.M. Karim, M.H. Engelhard, Z. Wei, D.L. King, Y. Wang, J. Catal. 287 (2012) 37–43.
- [33] T. Shishido, H. Asakura, F. Amano, T. Sone, S. Yamazoe, K. Kato, K. Teramura, T. Tanaka, Catal. Lett. 131 (2009) 413–418.
- [34] Y. Shimmi, S. Koso, T. Kubota, Y. Nakagawa, K. Tomishige, Appl. Catal. B: Environ. 94 (2010) 318–326.
- [35] A. Tougerti, S. Cristol, E. Berrier, V. Briois, C. La Fontaine, F. Villain, Y. Joly, Phys. Rev. B 85 (2012) 151536.
- [36] T. Komanoya, H. Kobayashi, K. Hara, W.-J. Chun, A. Fukuoka, Appl. Catal. A: Gen. 407 (2011) 188–194.
- [37] T. Komanoya, H. Kobayashi, K. Hara, W.-J. Chun, A. Fukuoka, ChemCatChem, in press, doi: 10.1002/cctc.201300731.
- [38] S.J. Tauter, Acc. Chem. Res. 20 (1987) 389–394.
- [39] E. Furimsky, Appl. Catal. A: Gen. 199 (2000) 147–190.
- [40] N. Akiya, P.E. Savage, Ind. Eng. Chem. Res. 40 (2001) 1822–1831.
- [41] B. Kuhlmann, E.M. Arnett, M. Siskin, J. Org. Chem. 59 (1994) 3098–3101.
- [42] M.J. Antal Jr., M. Carlsson, X. Xu, D.G.M. Anderson, Ind. Eng. Chem. Res. 37 (1998) 3820–3829.
- [43] N. Akiya, P.E. Savage, Chem. Rev. 102 (2002) 2725–2750.
- [44] X. Wang, R. Rinaldi, Angew. Chem. Int. Edit. 52 (2013) 11499–11503.